IEEE Sensors Letters VOL. 3, NO. 2, FEBRUARY 2019 6000104 IEEE Sensors Council

Sensor applications

A Paper-Based Inkjet-Printed Graphene Sensor for Breathing-Flow Monitoring

R. Lu[1], Mohammad R. Haider[1*], S. Gardner[1], J. I. D. Alexander[1], and Y. Massoud[2**]

[1]School of Engineering, University of Alabama at Birmingham, Birmingham, AL 35205 USA
[2]Stevens Institute of Technology, Hoboken, NJ 07030 USA
*Member, IEEE
**Fellow, IEEE

Manuscript received July 21, 2018; revised October 11, 2018; accepted November 28, 2018. Date of publication December 6, 2018; date of current version January 31, 2019.

Abstract—Continuous monitoring of breathing flow is an essential but often poorly utilized predictor that is causing poor patient outcome. A low-cost, light-weight, easy-to-use, reliable, and disposable breathing sensor is required to bypass the limitations of existing conventional sensors, which are bulky, expensive, and often require experts to handle. In this article, a low-cost, inkjet-printed graphene sensor on a disposable glossy photo-paper substrate is presented for breathing-rate monitoring. The sensor architecture consists of a graphene nanoparticle based thin functional layer on top of a silver nanoparticle based interdigitated conductive pattern. A standard office inkjet-printer was configured with nanoparticle inks and a printed circuit board design software was utilized for the layouts. The sensor was tested in a laboratory environment, and its data were analyzed for different breathing patterns. An empirical model of the sensor was developed using the Cole–Cole impedance model. Test results showed successful detection of breathing rates for different breathing patterns. The prototype sensor provides a low-cost, disposable, and practical solution for frequent breathing pattern recognition.

Index Terms—Sensor applications, breathing flow, graphene, inkjet-printing, paper substrate, breathing monitor, sensor.

I. INTRODUCTION

Breathing rate, in coordination with heart rate and blood temperature/pressure, is an essential vital sign when monitoring human health. A change in breathing pattern is a strong predictor of disease progression for chronic diseases such as cardiac arrest, chronic kidney disease, and muscular dystrophy [1]–[3]. In addition, an abnormal breathing pattern indicates risk of some underlying disease. For a healthy adult, a typical resting breathing frequency is 12–15 times/min. The associated carbon dioxide (CO_2) concentration during exhalation is 4%–5.3%, which is less than 1%, compared with inhalation. The difference in exhaled CO_2 concentrations at respiratory rates above or below normal conditions is correlated with the degree of physical discomfort or a health disorder [4]–[6].

Monitoring breathing rates both in and out of the hospital environment can enable early detection of abnormalities and subsequently trigger the timely initiation of emergency measures, ultimately saving lives. Fieselmann *et al.* [16] reported that a respiratory rate of 27 breaths/min (bpm) or more was the most important predictor of cardiac arrest in hospital wards. Cretikos *et al.* [17] found that just more than half of all patients suffering from a serious adverse event on the general wards (such as a cardiac arrest or ICU admission) had a respiratory rate greater than 24 bpm. Furthermore, it was also found that abnormal breathing rates could have been identified up to 24 h before the event.

Most current breathing measurements use pressure sensors to determine breathing patterns and function. They measure the difference between chest volumes during inhalation and exhalation. More pressure is exerted on the sensor during inhalation compared with exhalation [7]–[9]. The main drawback of pressure sensor measurements is the need for an additional equipment to suppress external forces (vibration, patient movement, etc.) that might interfere with the measurement. The resulting bulky setup typically results in patient discomfort and makes long-term continuous monitoring difficult. In addition, the cost limits widespread deployment and usage of pressure sensor measurements. An alternative method would be the use of acoustic sensors, which are low cost and easy to deploy [10], [11]. However, acoustic sensors are affected by noisy surroundings such as patients' coughs and inner-body sounds that may obscure the sensor signal.

This letter proposes a low-cost, light-weight, and disposable two-layer sensor that is printed on a glossy photo-paper substrate. The first layer uses a silver (Ag) nanoparticle ink to realize the interdigitated electrode pattern on photo-paper substrate. The second layer is a thin coating of graphene ink. The latter is sensitive to breathing temperature. The slight temperature difference between inhalation and exhalation creates a conductivity modulation of the graphene layer that can be monitored by external device. This simple structure provides a stable, low-cost, and easy-to-fabricate method of respiratory rate monitoring. The entire testing system consists of a breathing sensor tube (BST) with a printed sensor on the interior and a tablet/computer for data acquisition, breathing-pattern recognition, and display. The system level block diagram is shown in Fig. 1. A commercial office inkjet-printer was retrofitted with customized nanoparticle ink cartridges. Standard printed circuit board (PCB) design software was used to print the sensor onto glossy photo-paper.

The organization of this article is as follows. Sensor materials and structure are discussed in Section II. Sensor characterization using the Cole–Cole impedance model is discussed in Section III. Experimental results of the sensor testing and the conclusion are presented in Sections IV and V, respectively.

II. PROTOTYPE INKJET-PRINTED SENSORS

Printing electronics on flexible substrates are rapidly developing because of the ability to design multiplane electronics for functional

Corresponding author: Mohammad R. Haider (e-mail: mrhaider@uab.edu).
Associate Editor: O. Brand.
Digital Object Identifier 10.1109/LSENS.2018.2885316

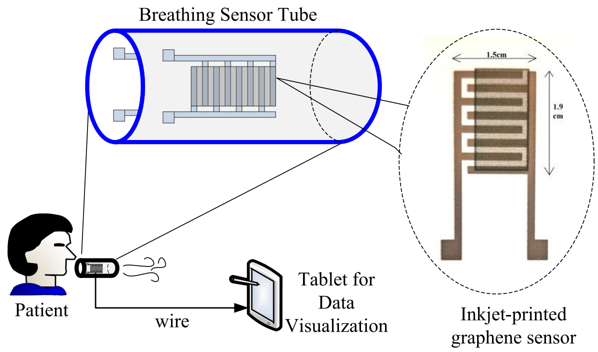

Fig. 1. Schematic overview of a breathing-rate monitoring system for remote usage. The inset shows the inkjet-printed graphene sensor mounted within the BST.

networks and low-cost fabrication. A printable sensor typically consists of three basic elements: 1) printing materials; 2) circuit structure; and 3) flexible substrates [12].

In general, the printing materials can be divided into three subcategories: 1) conductors; 2) semiconductors; and 3) dielectrics [14], [15]. In this article, superconducting nanoparticle silver (Ag) was chosen as the first (lower) layer because of its high thermal conductivity and low resistivity on photo-paper substrate. Silver has one valence electron that freely and easily moves into the holes of positively charged Ag atoms, thus resulting in extremely low resistance to current flow.

Semiconducting graphene was used as the second (upper) layer. Graphene is a single layer of sp^2-hybridized carbon atoms, where interacting atoms form two covalent hydrogen bonds. This causes extraordinarily high thermal and electrical conductivity. It has the thickness of an atom, which means it is transparent ($< 3\%$ visible light absorption), light, and flexible. Graphene has high carrier mobility [10^3– $10^6 \text{cm}^2/(\text{V} \times \text{s})$], density, conductivity (10^2–10^6 S/m), zero band gap, and very low resistivity. It is very sensitive to the surrounding environment based on its huge surface-to-volume ratio (2600 m^2/g). Even a single gas molecule can be detected by adsorption or release.

Standard PCB technology works well for most applications since high resolutions can be attained. Such technology is integrated into most modern circuits. There are several fundamental flaws of current PCBs. First, the physical realization of this technology is limited to a bulky and small-area device. As a result, post fabrication revisions are difficult to implement. Second, the manufacturing of PCBs is time consuming and costly. However, inkjet-printed circuits (iPC) open the field to more design freedom because of substrate flexibility, ease of editing/reprinting, wide array of ink materials, and low costs. While there are many potential applications of this emerging technology, there are many aspects of iPC performance that need improvement such as registration, electrode alignment, resolution, leakage current, and roll-to-roll processing [19].

Conductive inks are developed and characterized by material scientists and chemists. The ink is typically a mixture of metal nanoparticle, solvent, and surfactant. The surfactant serves to prevent the ink from coagulating and clogging the printer's nozzle head. Other properties of interest when developing these inks are liquid viscosity and surface tension. Quality of ink conductivity is affected by how the ink is spread on the substrate, which depends on droplet volume (printing resolution) in addition to wettability of the liquid [19]. A ring effect could occur as the ink dries, causing nonuniform dispersion and impaired conductivity [18]. These conditions are kept in mind while designing the inks and must be held to high standards of stability and performance for this emerging technology to flourish.

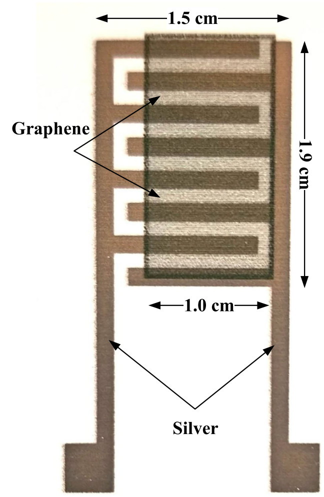

Fig. 2. Prototype inkjet-printed sensor. An interdigitated pattern is printed using silver nanoparticle ink and a thin coating of graphene material is utilized as a functional layer for sensing different environmental parameters.

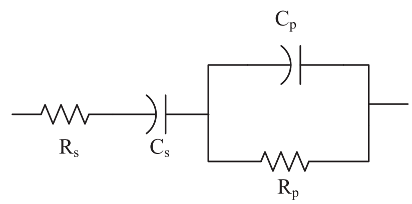

Fig. 3. Circuit schematic of second-order Cole–Cole model.

Prototype Fabrication: Flexible photo-paper was used as the sensor substrate in order to achieve low-cost, light-weight, and ease-of-fabrication goals. A standard desktop Brother printer, MFC-J5910, was configured by replacing the standard ink contents found in LC75 and LC27 cartridges with conductive metallic ink. The prototype inkjet-printed sensor is shown in Fig. 2. The sensor's dimensions were 1.9 cm × 1.5 cm; the covered graphene's dimensions were 1.9 cm × 1.0 cm, and the silver line width was 1.6 mm. Conductive metallic inks were procured from Millipore Sigma and then placed into emptied standard printer cartridges. A commercial PCB layout software, Easy-PC 12, was used to draw the structure layout. The layer thickness of each of the printed metallic inks was controlled by selecting different printing modes from the Brother printer utility software. In the prototype sensor investigated here, the silver and the graphene layers were printed using photo-print and ink-save print modes, respectively. This custom setup for inkjet-printing metallic inks obviates the need for expensive material printers (costing approximately \$50 K or more) usually used for inkjet-printing process.

III. MODELING AND CHARACTERIZATION OF PROTOTYPE SENSOR

The Cole–Cole impedance model is a widely popular method for determining the dielectric constant and impedance characteristics of biomaterials. The prototype sensor can be represented by Cole–Cole impedance model. A circuit schematic of the Cole–Cole impedance model [13] is shown in Fig. 3.

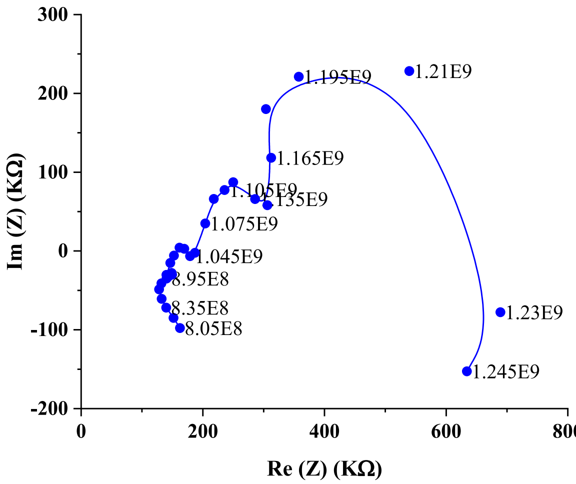

Fig. 4. Impedance diagram under pure nitrogen. The data labels show different frequencies.

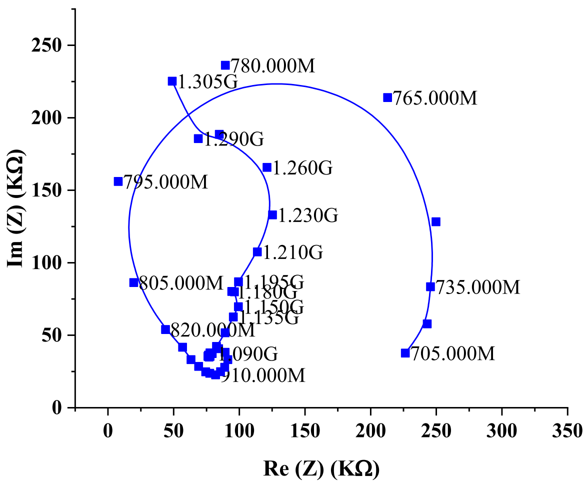

Fig. 5. Impedance diagram under atmosphere containing nitrogen and 2% CO_2. The data labels show different frequencies.

The total impedance Z of the electrical equivalent circuit model is given as follows:

$$Z(\omega) = R_s + \frac{R_p}{1+\omega^2 C_p^2 R_p^2} - j\left(\frac{\omega C_p R_p^2}{1+\omega^2 C_p^2 R_p^2} + \frac{1}{\omega C_s}\right). \quad (1)$$

The variations of real part $R_s + \frac{R_p}{1+\omega^2 C_p^2 R_p^2}$ and imaginary part $\frac{\omega C_p R_p^2}{1+\omega^2 C_p^2 R_p^2} + \frac{1}{\omega C_s}$, with angular frequency ω, in the presence of environmental condition constitute the Cole–Cole impedance plots.

The sensor impedance was measured using an HP 4396B impedance analyzer. The measured frequencies ranged from 700 MHz to 1.3 GHz. The sensor was exposed to pure nitrogen and nitrogen with 2% CO_2, and the corresponding Cole–Cole plots are shown in Figs. 4 and 5, respectively. In both cases, the prototype sensor was followed a second-order Cole–Cole model, as shown in Fig. 3. All the experiments were conducted at room temperature (20 °C). In Figs. 4 and 5, apparent dual loop semicircles were visible from the measured data points. For example, in Fig. 5, for 910 MHz to 1.30 GHz, a second semicircle was formed, which corroborated the second-order Cole–Cole model of the prototype sensor. The presence of atmosphere containing pure nitrogen or CO_2 changed the dielectric constant and conductivity, thus shifting the center of the semicircle. The R_s and C_s components (see Fig. 3) made the shifts in x-direction and y-direction, respectively. The R_p and C_p components had significant contributions to the change in radius of the semicircle.

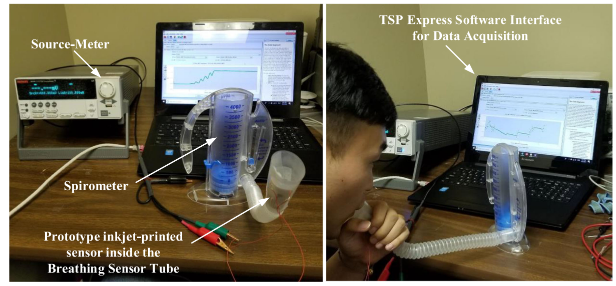

Fig. 6. Test setup of the prototype inkjet-printed sensor with a commercial spirometer. A student volunteer performed constant-volume-breathing by observing the spirometer reading, and the corresponding sensor resistance variations were recorded by the source-meter.

IV. TEST RESULTS

The prototype sensor was mounted inside a transparent plastic tube with openings at both ends to ensure smooth breathing-air flow. The plastic tube was approximately 3 inch long and 1 inch in diameter, and is referred to in this letter as "BST" (see Fig. 1). The prototype sensor was glued to the interior wall of the tube while keeping the printed nanoparticle layers exposed to the internal tube air. The two copper wires connected to the sensor were drawn out of the tube and connected to the probe leads of a measuring device. The BST was attached to a commercial spirometer (see Fig. 6) to monitor the sensor performance with constant-volume breathing pattern.

A high-precision source-meter, Keithley 2635 A, was used to monitor impedance variations of the graphene sensor in coordination with the breathing rate. A TSP Express software interface was utilized to directly acquire the data from source-meter to Excel file. A student volunteer breathed through the BST, and the corresponding data were recorded in the Excel files. A voltage limit of 12 V was set up in the source-meter to allow current flow through the prototype sensor, and the corresponding resistance change was measured by the source-meter device.

Short-Term Breathing Test: Since the prototype sensor is sensitive to both temperature and humidity, the volunteer breathed through the BST approximately 3 inch away from the prototype sensor. The BST was attached to the breathing tube of a commercial spirometer, and the student volunteer breathed repetitively for a fixed duration with a near-constant breathing-volume by observing the spirometer reading. All the breathing tests were conducted for a duration of 50 s. The student volunteer performed the tests for three different breathing-volumes, and the corresponding test results are shown in Fig. 7. As is evident from the figure, for different constant-volume breathing patterns, the prototype sensor successfully detected the breathing rates.

Long-Term Breathing Test: For long-term stability and reliability assessment of the sensor, the prototype sensor in this article was used for two weeks: twice a day and for 20 min each time. A Keithley 2635 A high-precision source-meter was used to measure the current through the sensor. For the test, the DC voltage limit of the source-meter was 12 V, and the room temperature was approximately 20 °C. The resistance variation of the sensor with time is shown in Fig. 8.

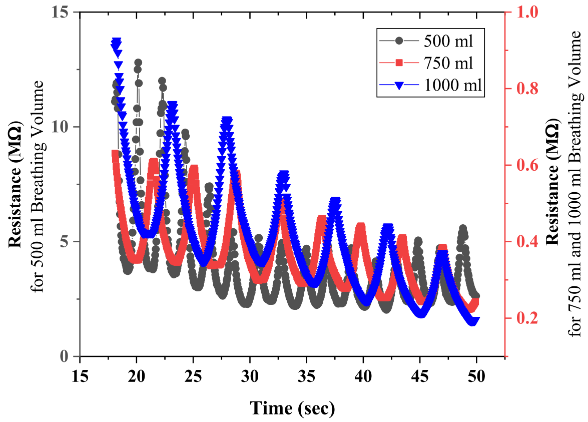

Fig. 7. Test results of sensor resistance variation for repetitive breathings of different constant volumes of atmospheric air.

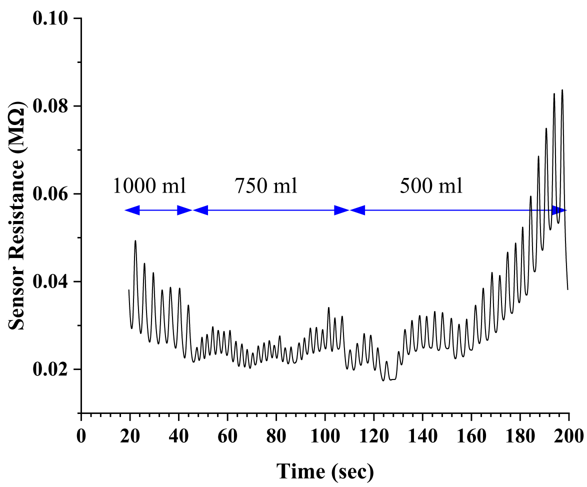

Fig. 8. Test result of sensor resistance variation with time for different volumes of breathing patterns.

The test also combined three different constant-volume breathing patterns. During the test period, the sensor had been reset before every test by a small puff (2–3 s) of hot air having 100 °C or more temperature. After every reset, the prototype sensor returned to normal operating mode while going through three to seven transition periods. The sensor was intended for disposable and short-duration operation. As shown in Fig. 8, even without reset, the sensor successfully performed for more than 200 s, which is good enough for any breathing test. Based on the test results, the sensor accurately identified each breathing pattern after prolonged use. The experimental results showed that the prototype inkjet-printed graphene sensor can work reliably for extended periods.

V. CONCLUSION

In this article, a silver and graphene nanoparticle based sensor for breathing-rate monitoring is demonstrated by inkjet-printing on glossy photo-paper. Fabricated using a standard office inkjet-printer, the prototype sensor offers a low-cost, light-weight, and environment-friendly sensor for mass-scale deployment and multiple applications. Test results showed stable performance of the sensor under different breathing patterns. The Cole–Cole model verified the impedance characteristics of the prototype sensor. The prototype sensor offers reduced manufacturing costs in the lab environment, ease of integration, and user comfort for wearable device development.

ACKNOWLEDGMENT

The work was supported in part by National Science Foundation (NSF) Award CNS-1645863 and Award ECCS-1813949.

REFERENCES

[1] M. A. Rusli and S. Takayama, “Jog training coaching assistance based on vital signs evaluation,” in *Proc. 56th Annu. Conf. Soc. Instrum. Control Eng. Jpn.*, Kanazawa, Japan, 2017, pp. 1553–1558.

[2] Y. Khan, A. E. Ostfeld, C. M. Lochner, A. Pierre, and A. C. Arias, “Monitoring of vital signs with flexible and wearable medical devices,” *Adv. Mater.*, vol. 28, no. 22, pp. 4373–4395, 2016.

[3] A. Dinculescu, C. Vizitiu, and V. VĂČleanu, “Combined thermal infrared and visual spectrum imaging novel methodology for astronauts’ psychophysiological assessment. Verification for respiration rate determination,” in *Proc. E-Health Bioeng. Conf.*, Sinaia, Romania, 2017, pp. 73–76.

[4] J. Ma, “Compressed sensing for surface characterization and metrology,” *IEEE Trans. Instrum. Meas.*, vol. 59, no. 6, pp. 1600–1615, Jun. 2010.

[5] M. Berggren *et al.*, “Paper electronics and electronic paper,” in *Proc. 1st Int. IEEE Conf. Polymers Adhesives Microelectron. Photon. Incorporating POLY, PEP Adhesives Electron.*, Potsdam, Germany, 2001, pp. 300–303.

[6] M. R. Chaharmir, J. Ethier, D. Lee, and J. Shaker, “Design of dual-band frequency selective surfaces to block Wi-Fi using printable electronics technology,” in *Proc. 17th Int. Symp. Antenna Technol. Appl. Electromagn.*, Montreal, QC, Canada, 2016, pp. 1–3.

[7] X. Zhu, W. Chen, T. Nemoto, K. I. Kitamura, and D. Wei, “Analysis of pulse rate, respiration rhythm, and body movement during sleep detected by pressure sensor,” in *Proc. 2nd Int. Symp. Aware Comput.*, Tainan, Taiwan, 2010, pp. 213–219.

[8] S. Brady, L. E. Dunne, R. Tynan, D. Diamond, B. Smyth, and G. M. P. O’Hare, “Garment-based monitoring of respiration rate using a foam pressure sensor,” in *Proc. 9th IEEE Int. Comput. Wearable Comput.*, 2005, pp. 214–215.

[9] A. Valipour and R. Abbasi-Kesbi, “A heartbeat and respiration rate sensor based on phonocardiogram for healthcare applications,” in *Proc. Iranian Conf. Elect. Eng.*, Tehran, Iran, 2017, pp. 45–48. doi: 10.1109/IranianCEE.2017.7985502

[10] A. Jin, B. Yin, G. Morren, H. Duric, and R. M. Aarts, “Performance evaluation of a tri-axial accelerometry-based respiration monitoring for ambient assisted living,” in *Proc. Annu. Int. Conf. IEEE Eng. Med. Biol. Soc.*, Minneapolis, MN, USA, 2009, pp. 5677–5680.

[11] W. R. McGillis, C. Langdon, A. J. Williams, and B. Loose, “O2-MAVS: An instrument for measuring oxygen flux,” in *OCEANS*, Biloxi, MS, USA, 2009, pp. 1–9.

[12] A. Gordon, G. W. Roberts, and C. J. Fayomi, “Low-cost trimmable manufacturing methods for printable electronics,” in *Proc. IEEE Int. Symp. Circuits Syst.*, Montreal, QC, Canada, 2016, pp. 870–873.

[13] A. Santorelli and J. Schwartz, “Predicting Cole-Cole parameters of microfluids with microstrip technology,” in *Proc. IEEE Sensors Appl. Symp.*, Queenstown, New Zealand, 2014, pp. 219–222.

[14] W. Y. Chang, T. H. Fang, H. J. Lin, Y. T. Shen, and Y. C. Lin, “A large area flexible array sensors using screen printing technology,” *J. Display Technol.*, vol. 5, no. 6, pp. 178–183, Jun. 2009.

[15] H. Jiang, S. Arabi, H. Shahbazbegian, J. N. Patel, and B. Kaminska, “Inkjet printed optically variable devices on a polymer substrate patterned with nanopillar array structural pixels,” in *Proc. IEEE 15th Int. Conf. Nanotechnol.*, Rome, Italy, 2015, pp. 1394–1397.

[16] M. Cretikos *et al.*, “The objective medical emergency team activation criteria: A case–control study,” *Resuscitation*, vol. 73, pp. 62–72, 2007.

[17] J. F. Fieselmann *et al.*, “Respiratory rate predicts cardiopulmonary arrest for internal medicine patients,” *J. Gen. Internal Med.*, vol. 8, pp. 354–360, 1993.

[18] V. Correia *et al.* “Design and fabrication of multilayer inket-printed passive components for printed electronics circuit development,” *J. Manuf. Processes*, vol. 31, pp. 364–371, Jan. 12, 2018.

[19] S. Mandal, G. Purohit, and M. Katiyar, “Inkjet-printed organic thin film transistors: Achievements and challenges,” *Mater. Sci. Forum*, vol. 736, pp. 250–274, Jan. 18, 2018.